Görtler vortices in boundary layers with streamwise pressure gradient: Linear theory

Pascal Goulpié,[a] Barbro G. B. Klingmann,[b] and Alessandro Bottaro[c]
IMHEF-DGM, Ecole Polytechnique Fédérale de Lausanne, CH-1015 Lausanne, Switzerland

(Received 18 November 1994; accepted 17 October 1995)

Linear theory is used to analyze the stability of two-dimensional boundary layer flows to stationary Görtler vortices. The basic flow profiles in the boundary layer are described by the Falkner–Skan similarity solutions. We approach the problem both with local linear theory (with the streamwise position held fixed) and with a streamwise marching technique (to represent the evolution of the inlet disturbance). Comparisons of solutions obtained by the two methods are presented: The results are consistent in showing that adverse pressure gradients are destabilizing, as in the case of Tollmien–Schlichting waves. This is at odds with recent findings by Otto and Denier and underscores the sensitivity of the results to initial conditions.
[S1070-6631(96)01702-3]

I. INTRODUCTION

The topic of the linear growth of longitudinal vortices in a boundary layer developing along a rigid, curved surface is worthy of attention because of its technological relevance. In turbomachineries, for instance, the boundary-layer Reynolds number may be fairly low and the stability of the laminar flow might be important to determine the efficiency of the application in question. In such situations the base flow is three dimensional and subject to pressure gradients. A recent paper by Otto and Denier[1] analyzed, via a nonlocal linear stability analysis, the effect of cross-flow and pressure gradient on Görtler vortices developing along a concave wall of constant radius of curvature, in a parameter space of interest for practical situations. A previous theory,[2] in the asymptotic limit of large G (G denotes the Görtler number, an appropriate combination of the Reynolds number and a curvature parameter) demonstrated that the presence of cross-flow in the underlying basic motion is such that the Görtler instability is superseded by the cross-flow vortex mechanism. Otto and Denier showed that for small magnitudes crossflows and for $G=O(1)$ the Görtler mechanism is still operational. Furthermore, they considered the effect of a longitudinal pressure gradient in the absence of cross-flow, to find that adverse pressure gradients were stabilizing. This is opposite to what Ragab and Nayfeh[3] found with a local stability approach. Ragab and Nayfeh even reported that for decelerated boundary layers (before the occurrence of separation) there is a range of wave numbers for which instability occurs at all G's. The present paper aims at elucidating the problem of the stability of Görtler vortices in a two-dimensional boundary layer, subject to streamwise pressure gradients. Since it might appear that the discording conclusions available in the literature originate from the local or nonlocal nature of the stability approach, we will start with a brief review of the different techniques available for the analysis.

Local theories for the stability of the Blasius flow with respect to streamwise vortices started with Görtler.[4] His analysis was later extended by Hammerlin,[5] Smith,[6] Ragab and Nayfeh,[3] and Floryan and Saric.[7] All of these investigators formulated the problem by fixing the streamwise position, hence neglecting the variation of the mode function of the perturbation with streamwise distance. Because of different levels of approximation (for example, parallel or nonparallel base flows) the results differed, sometimes widely. Hall[8] was the first to approach the problem correctly by consistently taking into account the growth of the boundary layer. The stability equations he formulated were the same as Floryan and Saric's:[7] However, Hall abandoned the traditional eigenvalue solution technique and solved the parabolic equations directly by downstream marching, subject to some initial disturbance conditions. He clearly pointed out the nonexistence of a unique neutral curve and the dependence of the results on the shape of the initial perturbation and on the initial point of marching. Hall[9] also derived asymptotic equations in the large wave number and large G region and pointed out the uniqueness of the linear stability results in such a parameter space. Hall's conclusions received a mixed welcome in the transition–prediction community[10] since they seemed to preclude access to simple transition criteria of the e^n type. Day *et al.*[11] indicated that the results of the local nonparallel technique of Ref. 7 could be considered, in some asymptotic sense, as the limit to which the marching results tend some distance away from the leading edge. Far enough downstream, growth rates of linear Görtler vortices as a function of streamwise distance were found to be in good agreement between local and marching analyses, and similarly for the eigenfunctions. Problems arise in the determination of the first neutral point, before the collapse of marching and local curves of the spatial amplification factor. If the initial condition is taken from the solution of the local problem (an acceptable procedure, but not a necessary requirement), there is good accord between local and marching results for neutral stability. Conversely, the adoption of initial conditions such as those of Hall[8] and Otto and Denier[1] can

[a]Present address: LASEN-DGC, Ecole Polytechnique Fédérale de Lausanne, CH-1015 Lausanne, Switzerland.
[b]Present address: Volvo Aerospace Corp., Space Division, S-461 81 Trollhättan, Sweden.
[c]Corresponding author: Tel.: +41-21-693 3365; fax: +41-21-693 3646; e-mail:bottaro@dgm.epfl.ch

produce wide discrepancies in neutral curve prediction between the local and nonlocal approach. One should then determine whether the differences encountered stem uniquely from the different initial conditions chosen, or whether other factors hold some importance.

II. FORMULATION

The Navier–Stokes and continuity equations in cylindrical coordinates (r,θ,ζ) are the starting point of our analysis. We consider a boundary layer flow over a concave wall with constant radius of curvature $R, R\to\infty$. If l is a typical length along the wall and U_l is the value of the free-stream velocity that refers to l, the dimensionless boundary layer coordinates x, y, and z can be introduced via the equations

$$x=\frac{\theta R}{l},\quad y=-\frac{(r-R)}{l}\,\mathrm{Re},\quad z=\frac{\zeta}{l}\,\mathrm{Re}, \tag{1}$$

where $\mathrm{Re}=U_l\delta/\nu\gg 1$ is the Reynolds number, with $\delta=(\nu l/U_l)^{1/2}$ and ν the kinematic viscosity. The velocity components (v_r, v_θ, v_ζ) and the pressure p are made nondimensional and expanded in terms of the small parameter Δ as follows:

$$\begin{aligned}
&\frac{v_r}{U_l}\,\mathrm{Re}=-[V(x,y)+\Delta v(x,y,z)+O(\Delta^2)],\\
&\frac{v_\theta}{U_l}=U(x,y)+\Delta u(x,y,z)+O(\Delta^2),\\
&\frac{v_\zeta}{U_l}\,\mathrm{Re}=\Delta w(x,y,z)+O(\Delta^2),\\
&\frac{p}{\rho U_{l^2}}\,\mathrm{Re}^2=P(x)\mathrm{Re}^2+p_0(x,y)+\Delta p(x,y,z)+O(\Delta^2),
\end{aligned} \tag{2}$$

with ρ being the density. Substituting into the steady Navier–Stokes and continuity equations, grouping together all terms proportional to the same power of Δ, and neglecting terms of order Re^{-2} and smaller, we find at order $O(1)$,

$$U_x+V_y=0, \tag{3a}$$

$$UU_x+VU_y=-P_x+U_{yy}, \tag{3b}$$

$$UV_x+VV_y=-p_{0y}+V_{yy}-(GU)^2; \tag{3c}$$

at order $O(\Delta)$,

$$u_x+v_y+w_z=0, \tag{3d}$$

$$Uu_x+Vu_y+uU_x+vU_y=u_{yy}+u_{zz}, \tag{3e}$$

$$Uv_x+Vv_y+uV_x+vV_y=-p_y+v_{yy}+v_{zz}-2G^2Uu, \tag{3f}$$

$$Uw_x+Vw_y=-p_z+w_{yy}+w_{zz}, \tag{3g}$$

with the Görtler number $G=O(1)$ defined by

$$G^2=\frac{l}{R}\,\mathrm{Re}. \tag{4}$$

The leading-order equations (3a) and (3b) allow the determination of the basic flow and pressure fields (U,V,P). Equation (3c) is not used; it shows that a normal gradient of p_0 is set up to balance the centrifugal term $(GU)^2$. A self-similar boundary layer solution can be obtained for the general case of nonzero streamwise pressure gradients by assuming the outer flow to vary as x^m, and by enforcing no-slip conditions at the wall. This procedure yields the well-known Falkner–Skan similarity solution, so that a nondimensional streamfunction $f(\eta)$ satisfying the ordinary differential equation,

$$f'''+\tfrac{1}{2}(m+1)ff''+m(1-f'^2)=0, \tag{5}$$

with boundary conditions

$$f=f'=0,\quad \text{at}\quad \eta=0, \tag{6a}$$

$$f'=1,\quad \text{at}\quad \eta\to\infty, \tag{6b}$$

is sought. The similarity variable η is defined by

$$\eta=yx^{(m-1)/2}, \tag{7}$$

and the velocity components U and V are given by

$$U=x^m f', \tag{8a}$$

$$V=x^{(m-1)/2}\left(\frac{1-m}{2}\,\eta f'-\frac{1+m}{2}\,f\right). \tag{8b}$$

For $m=0$ the Blasius solution is recovered. Some Falkner–Skan solutions are shown in Fig. 1; $m=-0.0904$ corresponds to the limiting case of decelerating flow without separation at the wall. For accelerated flows the Falkner–Skan solutions obtained are unique for each m; for decelerating flows with $-0.0904<m<0$, there are infinite solutions available, the laminar wall jet in an external stream being an example.[12] Although such flows are of interest, we have chosen to focus here only on the classical solutions, where U monotonically increases with η. The Görtler instability of wall jets has been recently studied by Matsson.[13]

Equations (3d)–(3g) define the linear stability problem for the leading-order perturbations (u,v,w) and for p. The boundary conditions appropriate to (3d)–(3g) are

$$u=v=w=0,\quad \text{at}\ y=0\quad \text{and}\quad y\to\infty. \tag{9}$$

III. LINEAR STABILITY THEORY

A. Local approach

When a perturbation of the form $\tilde{f}(y)\exp(\sigma x+i\beta z)$ is superimposed on the Falkner–Skan profile, the disturbance equations become

$$\sigma\tilde{u}+D\tilde{v}+i\beta\tilde{w}=0, \tag{10a}$$

$$\sigma U\tilde{u}+U_x\tilde{u}+VD\tilde{u}+U_y\tilde{v}=D^2\tilde{u}-\beta^2\tilde{u}, \tag{10b}$$

$$\sigma U\tilde{v}+V_x\tilde{u}+VD\tilde{v}+V_y\tilde{v}=-D\tilde{p}+D^2\tilde{v}-\beta^2\tilde{v}-2G^2U\tilde{u}, \tag{10c}$$

$$\sigma U\tilde{w}+VD\tilde{w}=-i\beta\tilde{p}+D^2\tilde{w}-\beta^2\tilde{w}, \tag{10d}$$

where σ is the spatial growth rate of the vortices, β is the spanwise wave number, and D denotes differentiation with respect to y. The local, nonparallel linear stability eigenvalue problem is derived by equating the current streamwise loca-

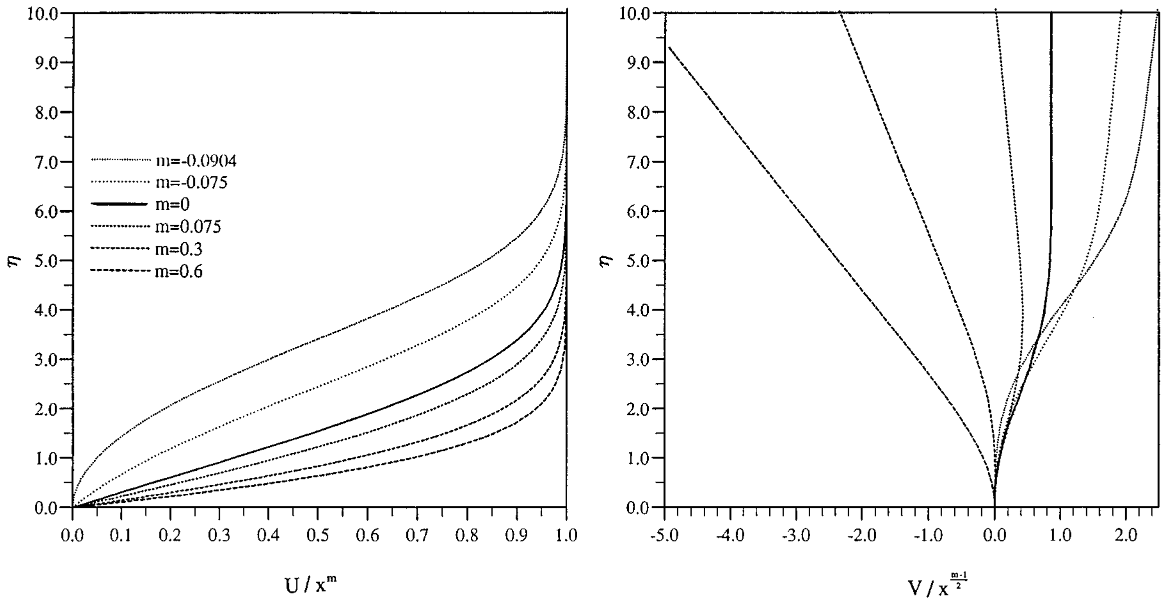

FIG. 1. Profiles of the basic flow velocity components for a variety of m's.

tion to the length scale l, i.e. setting $x=1$ and $\eta=y$. The pressure and $\tilde{w}$ are eliminated, and one finally arrives at a system of equations of the form

$$\mathbf{L}(\sigma,\beta,G)\tilde{f}=0, \tag{11a}$$

$$\mathbf{L}=\begin{bmatrix} L_{11} & L_{12} \\ L_{21} & L_{22} \end{bmatrix}, \quad \tilde{f}=\begin{bmatrix} \tilde{v} \\ \tilde{u} \end{bmatrix}. \tag{11b}$$

The spatial stability problem consists in determining σ for given values of β as function of G. The components of the linear operator $\mathbf{L}$ are

$$L_{11}=-(D^2-\beta^2)^2+V(D^2-\beta^2)D+V_y(D^2-\beta^2) + \sigma U(D^2-\beta^2)-\sigma U_{yy}, \tag{12a}$$

$$L_{12}=-\beta^2 V_x-2\beta^2 G^2 U+\sigma(V_y D+V_{yy}), \tag{12b}$$

$$L_{21}=U_y, \tag{12c}$$

$$L_{22}=-(D^2-\beta^2)+VD-V_y+\sigma U, \tag{12d}$$

and the boundary conditions (9) become

$$\tilde{u}=\tilde{v}=D\tilde{v}=0, \quad \text{at } y=0 \quad \text{and} \quad y\rightarrow\infty. \tag{12e}$$

By dropping all nonparallel terms in Eqs. (12a)–(12d), the original Görtler equations are retrieved:

$$L_{11}=-(D^2-\beta^2)^2+\sigma U(D^2-\beta^2)-\sigma U_{yy}, \tag{13a}$$

$$L_{12}=-2\beta^2 G^2 U, \tag{13b}$$

$$L_{21}=U_y, \tag{13c}$$

$$L_{22}=-(D^2-\beta^2)+\sigma U. \tag{13d}$$

B. Marching approach

The following analysis for the nonlocal approach follows closely the one given by Bertolotti[14] for the Orr–Sommerfeld case. The perturbation quantities are assumed to have the form

$$f(x,y,z)=\tilde{f}(x,y)\exp\left(\int \boldsymbol{\sigma}(x)dx+i\beta z\right). \tag{14}$$

The new feature compared to the local analysis is that the mode function $\tilde{f}$ is allowed to depend on x. The double dependence of f on x (both through $\boldsymbol{\sigma}$ and through $\tilde{f}$) is resolved by letting $\partial\tilde{f}/\partial x$ contain only changes in the mode shape, whereas the downstream growth of the perturbation is transferred to $\boldsymbol{\sigma}$. The x dependence of $\tilde{f}$ and $\boldsymbol{\sigma}$ is relatively weak, but comparable to the x dependence of the basic flow. Hence, when streamwise diffusion terms are present in the governing equations (such as for the Orr–Sommerfeld case), x derivatives of $\boldsymbol{\sigma}$ of all orders and x derivatives of $\tilde{f}$ of orders larger than unity, can be consistently neglected.[14] No particular procedure needs to be applied in the present case, since the linearized boundary layer equations (3c)–(3g) are the starting point of our analysis. On substitution of (14) into Eqs. (3c)–(3g), and after some algebraic manipulations, a parabolic system of equations of the form

$$\mathbf{L}\tilde{f}+\mathbf{M}\frac{\partial\tilde{f}}{\partial x}=0, \tag{15}$$

is obtained. The 2×2 linear operator matrices $\mathbf{L}$ and $\mathbf{M}$ are given by

$$L_{11}=-(D^2-\beta^2)^2+V(D^2-\beta^2)D+V_y(D^2-\beta^2) + V_{yy}D+V_{yyy}+\boldsymbol{\sigma}U(D^2-\beta^2)-\boldsymbol{\sigma}U_{yy}, \tag{16a}$$

$$L_{12}=-V_x(D^2+\beta^2)-2\beta^2G^2U$$
$$+2\boldsymbol{\sigma}(V_yD+V_{yy})+V_{xyy}, \tag{16b}$$
$$L_{21}=U_y, \tag{16c}$$
$$L_{22}=-(D^2-\beta^2)+VD-V_y+\boldsymbol{\sigma}U, \tag{16d}$$
$$M_{11}=U(D^2-\beta^2)-U_{yy}, \tag{16e}$$
$$M_{12}=2(V_yD+V_{yy}), \tag{16f}$$
$$M_{21}=0, \tag{16g}$$
$$M_{22}=U. \tag{16h}$$

Note that here **L** is different from the local one. This is because in the local analysis the mode shape assumption is introduced directly into the original system of equations; subsequently $\tilde{p}$ and $\tilde{w}$ are eliminated. This is the same procedure as, e.g., Floryan and Saric.[7] In the marching analysis, a two-equation set is first derived through elimination of p and w; then (14) is used. It should also be pointed out[15] that a local problem with **L** as by (16a)–(16d) produces results almost indistinguishable from those of the original local problem (12a)–(12d).

III. NUMERICAL PROCEDURE

The equations are solved by a spectral method, with $\tilde{f}$ decomposed into Chebyshev polynomials. The domain (y: $0\rightarrow\infty$) is mapped onto (y_T: $-1\rightarrow 1$) by the transformation

$$y_T=1-2e^{-y/y_0}, \tag{17}$$

where y_0 is a parameter that defines the clustering of points and is taken between 15 and 50. The Chebyshev polynomial are evaluated at the collocation points

$$y_T=-\cos\frac{j\pi}{M+1}, \quad j=0,\ldots,M, \tag{18}$$

and M is the number of collocation points (typically 80). The local eigenvalue problem is solved using a QZ algorithm from the NAG library; the code has been validated through extensive comparisons against the results of Floryan and Saric[7] and those of Zebib and Bottaro[16] for the case of Görtler vortices with system rotation. The marching equations are discretized in x with a second-order accurate finite difference scheme, and have been validated against results obtained from a different finite volume code.[17]

In the local code, the amplification rate σ is obtained directly from the equations; in the marching procedure a local amplification rate can be defined as

$$\tilde{\sigma}=\frac{\Delta E}{E\ \Delta x}, \tag{19}$$

where E is a chosen measure of the amplitude of the perturbation. At each x step the energy growth is transferred to the exponential term and $\boldsymbol{\sigma}$ is updated in such a way that the amplitude is unchanged, i.e.

$$\frac{\partial E}{\partial x}=0; \tag{20}$$

this is also called the normalization condition.[14] Because of the scalings adopted, the locally scaled amplification rate is

$$\sigma=\tilde{\sigma}x. \tag{21}$$

Several choices of E are possible. A common (and *a priori* reasonable) choice is to take

$$E=\frac{1}{A}\int_A u^2\ dA, \tag{22a}$$

with A the cross section. In this case E represents the perturbation energy; v and w are not included because they are one Re order of magnitude smaller. Note, however, that E defined by (22a) can grow algebraically for small x's in the absence of the driving term ($G\equiv 0$) because of the "lift-up effect."[18] Conversely, both cross-stream perturbation velocity components are damped at all values of x.[19] Because of the algebraic "instability," criterion (22a) could have the effect of indicating growth in an x range where vortices are decaying. Hence, the adoption of a criterion based on v and/or w and/or the streamwise vorticity could be more appropriate to represent growth or decay of streamwise vortices. We have thus chosen an alternative criterion, with E defined by

$$E=\frac{1}{A}\int_A v^2\ dA. \tag{22b}$$

In the following, the two criteria (22a)–(22b) will be referred to as the u criterion and the v criterion. They will both be adopted and compared. Obviously, other criteria are accessible and are equally valid/justifiable (Day *et al.*[11]).

All marching calculations are started from the initial location $x=1$, and as an initial value of the Görtler number G_0 we have chosen $G_0=0.5$ unless otherwise specified. At each downstream station x the local Görtler number is defined by

$$G=G_0x^{(3+m)/4}. \tag{23}$$

To trace curves of neutral stability in the $G-\beta$ plane, several nonlocal calculations must be carried out for a variety of initial values of the spanwise wave number β. By defining with β_0 the initial value of β, the locally scaled β becomes

$$\beta=\beta_0x^{(1-m)/2}. \tag{24}$$

The nondimensional wavelength Λ can also be introduced, via the relation

$$\Lambda=G\left(\frac{2\pi}{\beta}\right)^{3/2}. \tag{25}$$

Clearly, if at G_0 we have $\Lambda=\Lambda_0$ at the generic downstream station x, we have

$$\Lambda=\Lambda_0x^m, \tag{26}$$

and for $m=0$ we recover the well-known result that Λ remains unchanged downstream.

The choice of initial disturbance conditions for the marching calculations is especially crucial. We ideally wish to specify initial conditions that are physically sound and satisfy the governing equations; these conditions should represent the outcome of a complex receptivity process through which disturbances at the inlet of a test section, in the free

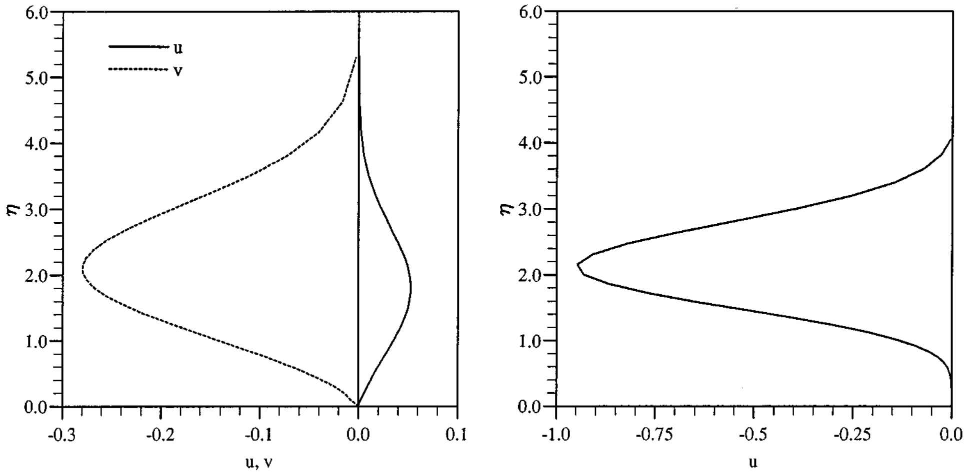

FIG. 2. Disturbance initial conditions for the present marching solutions (left) and for Hall's[8] case. In this latter case the (u,v) initial perturbations are given by $(\eta^6 e^{-\eta^2/\eta_{\text{ext}}},0)$ and η_{ext} has here been chosen equal to 2.

stream or at the wall, enter the boundary layer and are transformed into instability waves. The boundary layer approximation adopted is valid only sufficiently far downstream of the plate's leading edge; it is not unreasonable to think that at the streamwise distance l from which our calculations start, the receptivity of the flow has already operated on the disturbances to transform them into streamwise vortices of weak amplitude. The reason why streamwise vortices should be preferred to other possible forms of perturbations, in a flow case for which the instability is not yet operational (small G) lies in the fact that streamwise vortices represent the "optimal" perturbations[20] in the flat plate boundary layer flow ($G\equiv 0$). Optimal perturbations are those perturbations that attain maximum energy growth over a chosen space or time interval; this algebraic energy growth is transient and occurs despite the absence of exponential normal mode instability in the shear flow. In the present case streamwise vortices might be amplified initially by the "algebraic" instability when $G\rightarrow 0$; with the increase of x (and G), exponential amplification may be turned on by the forcing term $2G^2Uu$ in the vertical disturbance momentum equation.

Since there is no formal mathematical justification for adopting as initial conditions the eigenfunctions of the local stability problem, we have chosen to apply at the inlet of the calculation domain the perturbation velocities u and v shown in Fig. 2. Such velocity profiles represent near-wall vortices, and are constructed by solving the linear marching equations for $m=0$, $\Lambda=62$, from $G=1$ to $G=40$, starting from the local linear solution; the results obtained at $G=40$ are used as inlet conditions for all calculations performed. Although these initial perturbation velocity distributions are arbitrary, they are physically plausible. In Fig. 2 we have also represented the initial conditions proposed by Hall[8] and adopted in the study by Otto and Denier.[1] Although they are not "wrong," the absence of a vertical perturbation velocity component a finite distance downstream of the plate's leading edge makes them "unusual." The effect of Hall's initial conditions is that the perturbation will always relax in the initial phase until velocity distributions consistent with the governing equations are obtained; past this stage the spatial development of the vortices becomes the same as for more physical inlet velocity profiles.[21] Since the initial relaxation will be interpreted as a decay, it is expected that Hall's initial conditions will produce neutral points farther downstream (hence, for larger G) than other inlet distributions, for example, those based on the solution of the local problem. This has been verified by our calculations.

An alternative choice of starting conditions, which was proposed to us by a referee, could possibly be obtained directly from the governing equations appropriately reduced to a self-similar set of ordinary differential equations.[22] This would be particularly useful in the limit of small spanwise wave numbers, where local theories do not hold.

IV. RESULTS

A local analysis produces a unique neutral curve for each value of m. Results of nonlocal analyses are of more ambiguous interpretation if one has the objective of defining a neutral curve. The factors causing this ambiguity are examined below.

A. Factors affecting the determination of the neutral point in a nonlocal analysis

In Fig. 3 we have reported the locally scaled amplification factor σ as a function of G, for $m=0$, $\Lambda=62$, and for $G_0=0.5$, 1, and 2. The value of σ is based on the v criterion; similar results are achieved for σ based on u or other criteria and for different values of m and Λ_0. In all cases there is an initial phase in which σ decreases until a peak negative value is reached and the vortices are maximally damped; farther downstream, σ starts increasing and the vortices amplify. The neutral points, where the curves cross the $\sigma=0$ axis while in their ascending phase, are found at $G=3.8$, 5.3, and 7.4 in order of increasing G_0.

In Fig. 4, the influence of the criterion chosen for the definition of the neutral point is shown, for $m=0.05$, $G_0=0.5$, and $\Lambda_0=210$. For comparison purposes, the local

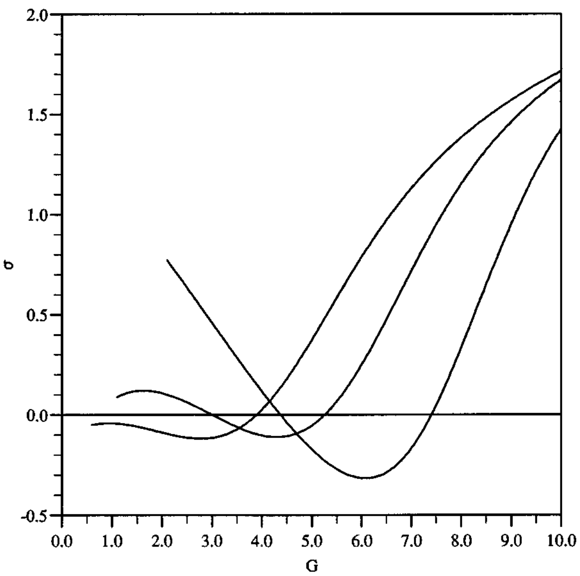

FIG. 3. Influence of the initial Görtler number G_0 on the first neutral point. Here $\Lambda=62$, $m=0$; the v criterion.

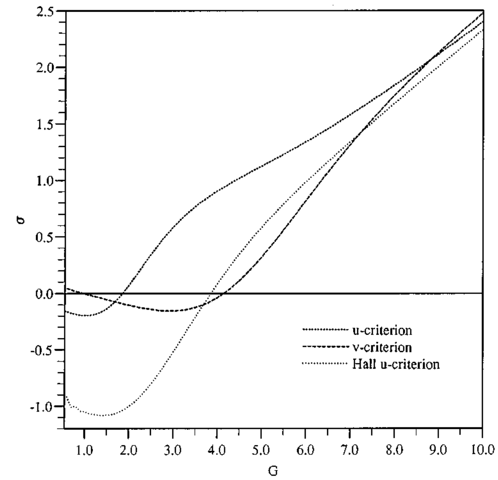

FIG. 5. Influence of the inlet condition on the first neutral point. Here $\Lambda_0=62$ at $G_0=0.5$, $m=0.05$.

curve is also plotted. The difference between the u and the v criteria in the definition of the neutral point appears immediately: The v criterion seems to indicate that for all $G>G_0$ vortices are amplified. On the other hand, according to the u criterion growth occurs only for $G>1.3$. Interestingly, the neutral point of the local nonparallel theory is contained in between these two predictions.

The last factor causing nonuniqueness in the definition of the neutral point is the initial condition used to initiate the marching. Its influence can be appreciated by inspection of Fig. 5, where a comparison of results obtained with the present initial conditions and with Hall's is presented. The case considered to illustrate our point corresponds to $\Lambda_0=62$, $m=0.05$. The u criterion predicts a neutral point at $G=1.8$ with our initial conditions and $G=3.8$ with Hall's initial conditions. If the v criterion is adopted, the neutral point is shifted toward even larger G's.

These ambiguous results leave one wondering about the effective importance of a neutral curve in this problem. It might be more appropriate to consider, instead of one marginal curve, curves of constant, and sufficiently large, amplification factor. In this latter case, all procedures are likely to produce results in good agreement with one another; however, in order to answer the question of whether acceleration of the base flow is stabilizing or not for Görtler vortices near their onset, one needs to turn toward the "neutral curve."

B. Neutral curves from local and marching analyses

To define a neutral curve based on the nonlocal equations, several calculations starting from different values of Λ_0 need to be carried out. Because of the arguments presented in the previous section, it is clear that whatever neutral curve one obtains, the result should be interpreted in a qualitative sense. Only the generic question, "Is acceleration of the basic flow stabilizing or not for Görtler vortices?" can be somehow addressed, and an equally valid (or ambiguous) answer is also accessible from the local equations. Still, we set out to pursue the task of defining nonlocal neutral curves, at least to check whether they are consistent with the results of the local theory. Figure 6 shows an example of calculations of the growth rates σ as a function of G for a variety of initial Λ_0, for $m=0.075$ and for the two criteria under consideration. For the u criterion (Fig. 6, left) neutral points can be easily defined; for the v criterion some cases exist for which Görtler vortices appear to be always amplified.

Some local nonparallel marginal stability curves in the $\beta-G$ plane are plotted in Fig. 7. The area above each curve is the area of instability to Görtler vortices for the specified value of m. The local calculations would seem to predict instability for arbitrarily small β and G when $m=-0.075$; it is, however, clear that such a conclusion is hasty and probably erroneous because of the limitations of any local ap-

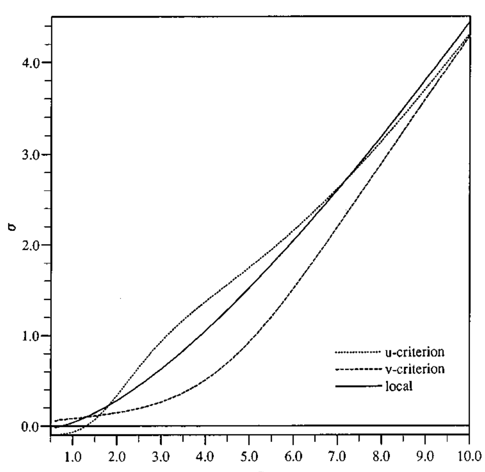

FIG. 4. Influence of the criterion used to define σ on the first neutral point, and comparison with the local nonparallel solution. Here $\Lambda_0=210$ at $G_0=0.5$, $m=0.05$.

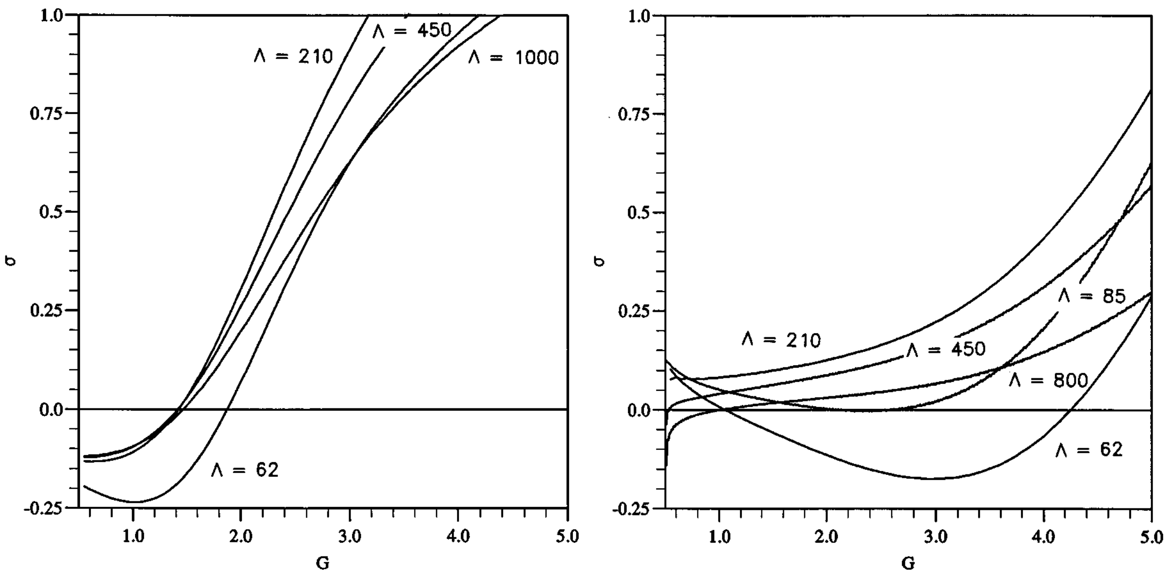

FIG. 6. Determination of the neutral points with the marching code for the two different criteria, $m = 0.075$.

proach there. Our results indicate that the unstable area increases with the decrease of m, for the $\beta - G$ range for which the equations are tenable. All the neutral curves intersect at $\beta \approx 2.2$ and $G \approx 11$; for $G > 11$, favorable pressure gradients become destabilizing, since the right branches of the neutral curves are moved progressively to the right. This behavior of the asymptotic large G regime was also noted by Otto and Denier.[1]

A summary of all the results obtained (local parallel and nonparallel, and marching) is presented in Fig. 8, and for comparison purposes the solutions of Otto and Denier[1] have been included. The local nonparallel marginal solutions agree with those of Ragab and Nayfeh,[3] including the sharp drop in the neutral curves for negative m's and low β's. Interestingly, for large negative m ($m = -0.075$) the u criterion for the nonlocal equations always indicates instability, and for $m = -0.05$ only neutral points in a very narrow β range can be found. For $m = \pm 0.075$ and ± 0.05 a range of wave numbers appears (contained between two oblique curves shown with thin solid lines) for which the v criterion predicts instability for all $G > G_0$. The presence of jumps in the nonlocal neutral curves must be ascribed to the initial condition chosen (and subsequent initial transient behavior of the solution) and to the initial Görtler number, from which the marching procedure is initiated. Different choices would have produced different neutral positions, reflecting the ambiguity of the problem and the existence of infinitely many "neutral curves." Keeping in mind the crucial importance of these factors, our results based on the u criterion and local results are consistent in showing that *deceleration is destabilizing*: With the decrease of m, the marginal curves are shifted toward lower values of G. The neutral points calculated by Otto and Denier[1] (with the u criterion) predict the opposite trend; we verified that the cause of this behavior stems from their choice of initial conditions.

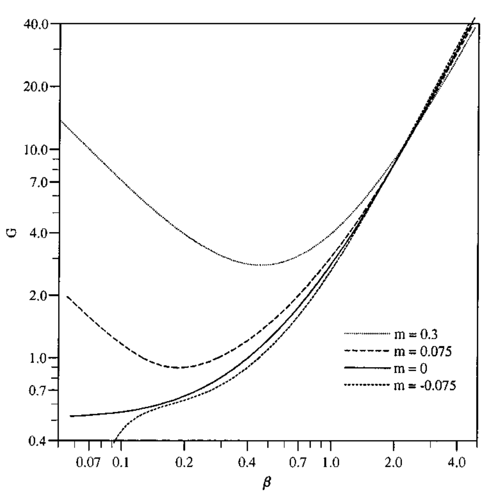

FIG. 7. Some local nonparallel neutral curves.

V. CONCLUDING REMARKS

The linear stability of Görtler vortices in accelerated and decelerated boundary layers of the Falkner–Skan family has been examined with local and nonlocal solution techniques. Whereas local analyses (parallel and nonparallel) predict a unique neutral curve for each base flow considered, nonlocal approaches yield a variety of marginal stability curves. This nonuniqueness stems from a variety of reasons, which have been examined in this paper: Initial conditions and the initial point where the conditions are applied, and criterion used to define a neutral point. Since discording results can be obtained, extreme care should be used to avoid hasty conclusions.

Both the local and marching results presented are consistent in showing destabilization of the flow under condi-

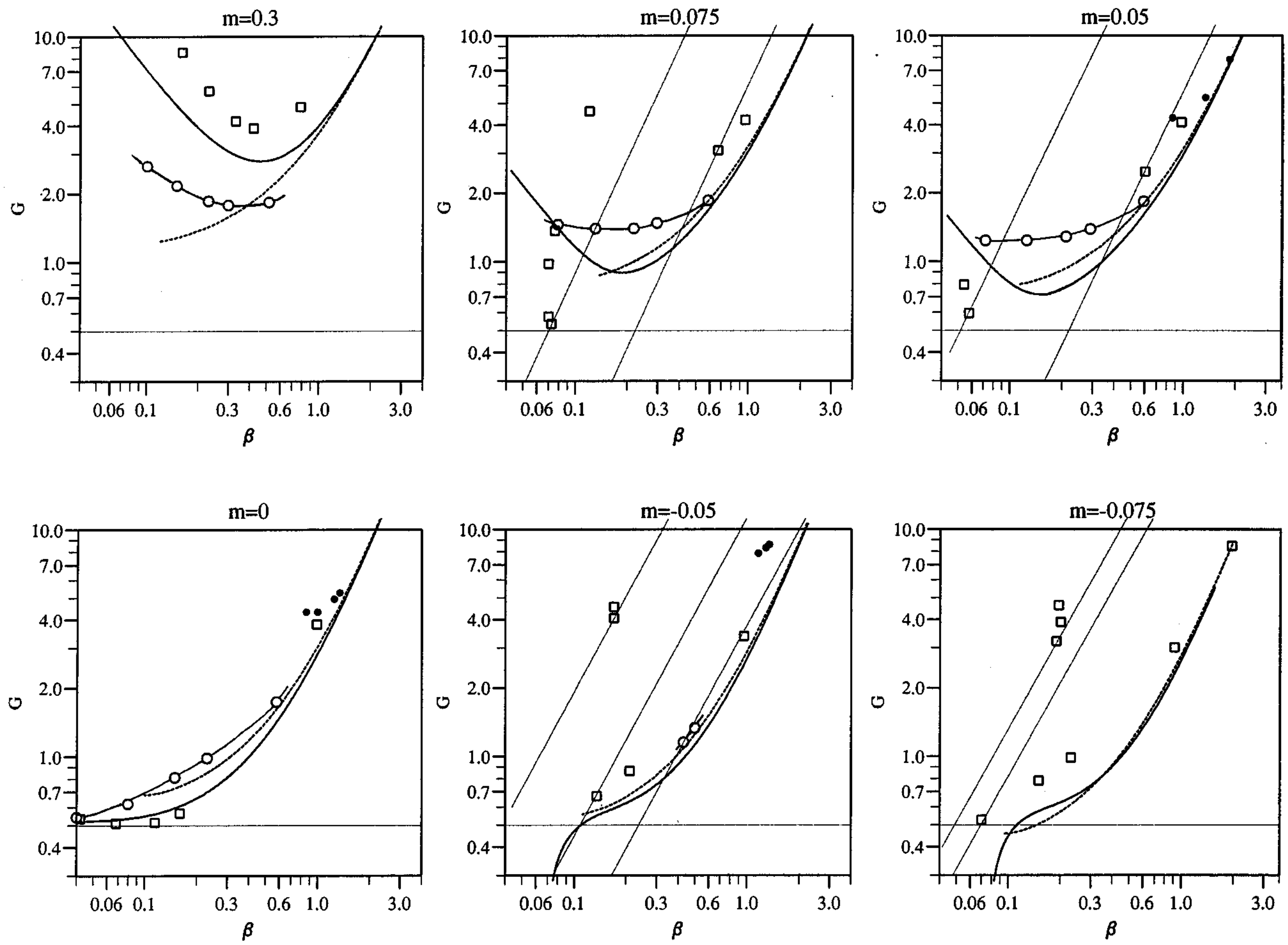

FIG. 8. Local and marching results. The continuous lines denote local, nonparallel marginal stability curves; dashed lines indicate local, parallel marginal stability curves. The neutral points according to the u criterion are denoted by empty circles and a solid line has been drawn to join these points; empty square symbols indicate $\sigma=0$ according to the v criterion. The full circles are the results by Otto and Denier.[1]

tions of adverse pressure gradients, and this is in line with linear stability results for the onset of Tollmien–Schlichting waves in boundary layers.[23] However, one can easily obtain the opposite result by a different choice of initial conditions; hence, the conclusions reached here should only be considered as indicative. A definite answer to the question of how pressure gradients affect the stability of Görtler vortices can be obtained only when receptivity calculations are used to supply the initial disturbance field.

ACKNOWLEDGMENTS

Support for this project has been provided by the Swedish Technical and Scientific Research Council and the Swiss National Fund, Grant No. 21-36035.92.

[1]S. R. Otto and J. P. Denier, "The effect of crossflow on Görtler vortices," ICASE Report No. 94-19 (submitted to J. Fluid Mech.)

[2]P. Hall, "The Görtler vortex instability mechanism in three-dimensional boundary layers," Proc. R. Soc. London Ser. A **399**, 135 (1985).

[3]S. A. Ragab and A. H. Nayfeh, "Effect of pressure gradients on the Görtler instability," AIAA Paper No. 80-1377, 1980; "Görtler instability," Phys. Fluids **24**, 1405 (1981).

[4]H. Görtler, "Uber eine dreidimensionale instabilität laminarer Grenzschichten an konkaven Wänden," Ges. d. Wiss. Göttingen, Nachr. Math. **2**, No. 1 (1940); H. Görtler, "Instabilität laminarer Grenzschichten an konkaven Wänden gegenüber gewissen dreidimensionalen Störungen," Z. Angew Math. Mech. **21**, 250 (1941) in English as NASA TM 1375, 1954.

[5]G. Hämmerlin, "Über das Eigenwertproblem der dreidimensionalen instabilität laminarer Grenzschichten ab konkaven Wänden," J. Rat. Mech. Anal. **4**, 279 (1955); "Zur theorie der dreidimensionalen instabilität laminarer grenzschichten," Z. Angew Math. Phys. **7**, 156 (1956).

[6]A. M. O. Smith, "On the growth of Taylor–Görtler vortices along highly concave walls," Q. Appl. Math. **13**, 233 (1955).

[7]J. M. Floryan and W. S. Saric, "Stability of Görtler vortices in boundary layers," AIAA Paper No. 79-1497, 1979 [appeared in revised version in AIAA J. **20**, 316 (1982).

[8]P. Hall, "The linear development of Görtler vortices in growing boundary layers," J. Fluid Mech. **130**, 41 (1983).

[9]P. Hall, "Taylor–Görtler vortices in fully developed or boundary layer flows: Linear theory," J. Fluid Mech. **124**, 475 (1982).

[10]V. Kalburgi, S. M. Mangalam, J. R. Dagenhart, and S. N. Tiwari, "Görtler instability on an airfoil," *NASA Symposium on Natural Laminar Flow and Laminar Flow Control Research*, NASA CP-2487, December 1987; V. Kalburgi, S. M. Mangalam and J. R. Dagenhart, "A comparative study of theoretical methods on Görtler instability," AIAA Paper No. 88-0407, 1988.

[11]H. P. Day, T. Herbert, and W. S. Saric, "Comparing local and marching analyses of Görtler instability," AIAA J. **28**, 1010 (1990).

[12]J. Steinheuer, "Similar solutions for the laminar wall jet in a decelerating outer flow," AIAA J. **6**, 2198 (1968).

[13]O. J. E. Matsson (private communication, 1994).

[14]F. P. Bertolotti, "Linear and nonlinear stability of boundary layers with

streamwise varying properties,'' Ph.D. thesis, The Ohio State University, Columbus, Ohio, 1991; also see F. P. Bertolotti, T. Herbert, and P. R. Spalart, ''Linear and nonlinear stability of the Blasius boundary layer,'' J. Fluid Mech. **242**, 441 (1992).

[15] B. G. B. Klingmann, ''Linear parabolic stability equations applied to three-dimensional perturbations in a boundary layer,'' IMHEF Report No. D-93-12, 1993.

[16] A. Zebib and A. Bottaro, ''Goertler vortices with system rotation: Linear theory,'' Phys. Fluids A **5**, 1206 (1993).

[17] A. Bottaro, B. G. B. Klingmann, and A. Zebib, ''Goertler vortices with system rotation,'' Theor. Comput. Fluid Dyn. (in press).

[18] M. T. Landahl, ''Wave breakdown and turbulence,'' SIAM J. Appl. Math. **28**, 735 (1975); ''A note on an algebraic instability of inviscid parallel shear flows,'' J. Fluid Mech. **98**, 243 (1980).

[19] A. Bottaro, ''On longitudinal vortices along curved passages,'' Workshop on Stability and Transition, Roslagens Pärla, Sweden, August 1993.

[20] K. M. Butler and B. F. Farrell, ''Three-dimensional optimal perturbations in viscous shear flow,'' Phys. Fluids A **4**, 1637 (1992).

[21] K. Lee and J. T. C. Liu, ''On the growth of mushroomlike structures in nonlinear spatially developing Goertler vortex flow,'' Phys. Fluids A **4**, 95 (1992).

[22] F. Bertolotti, ''Vortex generation and wave–vortex interaction over a concave plate with roughness and suction,'' ICASE Report No. 93-101, submitted to Theor. Comput. Fluid Dyn.

[23] P. G. Drazin and W. H. Reid, *Hydrodynamic Stability* (Cambridge University Press, Cambridge, 1981).